Physics Letters A 406 (2021) 127457

Contents lists available at ScienceDirect

Physics Letters A

www.elsevier.com/locate/pla

The spike state in type-I mesoscopic superconductor

Isaias G. de Oliveira [a,*], Leonardo R. Cadorim [b], Antonio R. de C. Romaguera [c], Edson Sardella [b], Rodolpho R. Gomes [d], Mauro M. Doria [d]

[a] Departamento de Física, Universidade Federal Rural do Rio de Janeiro, UFRRJ 23890-000, Seropédica, RJ, Brazil
[b] Departamento de Física, Faculdade de Ciências, Universidade Estadual Paulista (UNESP), Caixa Postal 473, 17033-360, Bauru, SP, Brazil
[c] Departamento de Física, Universidade Federal Rural de Pernambuco, UFRPE 52171-900 Recife, Pernambuco, Brazil
[d] Instituto de Física, Universidade Federal do Rio de Janeiro, UFRJ 21941-972 Rio de Janeiro, Brazil

ARTICLE INFO

Article history:
Received 9 April 2021
Received in revised form 14 May 2021
Accepted 22 May 2021
Available online 28 May 2021
Communicated by L. Ghivelder

Keywords:
Mesoscopic superconductor
Intermediate type-I superconductor
Genuine type-I superconductor
Spike state

ABSTRACT

We study here the spike state found in mesoscopic type I superconductors whose existence is confined to the single field where the superconducting state arises from the normal state in descending field in the so-called genuine type I regime. The mesoscopic type I superconductor possesses distinct κ regimes due to its richer critical field structure Cadorim et al. (2021) [11]. The lifetime of the spike state is shown to be in the nanosecond scale through the time dependent Ginzburg-Landau (TDGL) equations. The spike state is a giant vortex state that undergoes a process of deformation after its creation when several bubbles of vortices are expelled forming new but deformed giant vortices until no one is left inside the superconductor. Like phase slips and kinematic vortices, the spike state is also a non-equilibrium vortex state.

1. Introduction

The emergence of a finite resistance in superconducting wires was firstly observed in the seventies [1] and W. A. Little [2,3] proposed an interpretation as caused by a brief vanishing of the order parameter at some points along the wire. McCumber and Halperin [4] computed the characteristic time of this brief vanishing and found to fall in the range of 10 nanoseconds. This emergence of finite resistance has been the subject of research for decades and currently is known as phase slips [5], and understood to be a consequence of metastable vortex states. In other words the onset of resistance is due to the entrance and exit of fast vortices along the wire each one carrying a topological charge. Therefore phase slips can be regarded as topological fluctuations of the order parameter [5] observed in one-dimensional superconductors such as wires and rings. Nevertheless soon it was realized that this rapid motion of vortices along a superconductor also takes place in two-dimensional superconductors, and in this case they were called phase slip lines, which are rivers of fast vortices, also coined as kinematic vortices [6]. The phase-slip lines can be confused with possible local inhomogeneities in the films but to distinguish them low temperature scanning laser microscopy has been used to visualize them [7]. Clearly the study of phase-slips centers and lines is affected by the presence of pinning and inhomogeneities that obviously slow the motion of the fast vortices [8,9]. However the phenomena of phase-slips centers and lines lie beyond the existence of pinning. Indeed, through a nanoscale scanning superconducting quantum interference device [10] vortices were imaging showing their penetration at rates of tens of GHz revealing the formation of mesoscopic vortex rivers. From the theoretical side the study of phase slips and kinematic vortices is done in the context of the time dependent Gizburg-Landau theory (TDGL) [8–10].

In this paper, we study another metastable vortex state, hereafter called the spike state, that arises in the passage from the normal to the superconducting state of mesoscopic type I superconductors by lowering the applied field. To characterize it, we must consider the work of L. R. Cadorim et al. [11] showing that mesoscopic type-I superconductors undergo a transition in the coupling from *intermediate* to *genuine* regimes associated to the ranges $\kappa_{c1} < \kappa < 1/\sqrt{2}$ and $\kappa < \kappa_{c1}$, respectively. We numerically determine here the value of κ_{c1} for our object of study, a very long cylinder with fixed radius equal to $R = 6\xi$. The *intermediate* regime has distinct sub-regimes with a transition takes place from *paramagnetic* to *diamagnetic* behavior at the critical coupling κ_{c2} observed in the descending branch, which is also determined here. The spike state is a feature of the *genuine* regime and therefore arises for $\kappa < \kappa_{c1}$. No stable or unstable vortex configuration exists in the *genuine* regime whose the magnetic response is totally *diamagnetic* with the exception at the passage from the normal to the superconducting state. Exactly at the critical field that character-

* Corresponding author.
E-mail address: isaias@ufrrj.br (I.G. de Oliveira).

https://doi.org/10.1016/j.physleta.2021.127457
0375-9601/

izes this passage, and only there, a giant vortex state is created into the superconductor and immediately exits it. This is the spike state which is a metastable time dependent state, whose description and lifetime is estimated here and found to fall in the nanosecond range using the TDGL theory.

A clarifying nomenclature clarification becomes necessary at this point. Once only stationary states were investigated in Ref. [11], the time dependent nucleation and expulsion of vortices described above were not studied. In this manner, the spike state such as defined in the last paragraph could not have been found. Therefore, the term "spike state" was applied in Ref. [11] to define a totally different process, namely, the nucleation and subsequent expulsion of vortices over a very short interval of applied field values. In order to avoid confusion, hereafter, the term "spike state" is reserved solely to our previous definition of it, *i.e.*, the nucleation and *immediate* expulsion of vortices at a single value of the external field.

The κ_{c1} and κ_{c2} are intrinsic transitions of the superconductor associated to changes in the ordering of some critical fields. The existence of such kind of transition was firstly pointed out by M. Tinkham [12] and P. G. de Gennes [13] in their books who found that for the macroscopic superconductor takes place at $\kappa_c = 0.417$. To understand the Tinkham-de Gennes κ transition we review some of its key aspects below. A. Abrikosov [14] has shown more than fifty years ago that the Ginzburg-Landau (GL) coupling $\kappa = 1/\sqrt{2}$ splits the bulk superconductor into two classes, type-I and type-II, such that the latter kind possesses vortex solutions that have repulsive interactions. Many years later E. B. Bogomolny [15,16] showed that at this special coupling vortices cease to interact. The Abrikosov classification of bulk (without boundary) superconductors is well summarized by the expression relating two critical fields, $H_{c2} = \sqrt{2}\kappa H_c$, where H_{c2} is the upper critical field and H_c the thermodynamic field. Hence the type-I and II correspond to the situations $H_{c2} < H_c$ and $H_{c2} > H_c$, respectively. Nevertheless Saint-James and de Gennes [17] found that a surface substantially prolongs superconductivity beyond H_{c2} until another critical field H_{c3} is reached, whose value in case of a flat interface separating the superconductor to the external vacuum is $H_{c3} = 1.69H_{c2}$. H_{c3} has been the subject of theoretical and experimental research throughout the decades [18–23]. Thus the presence of an external boundary impacts the classification and novel situations arise for the type-I superconductor according to M. Tinkham [12] and P. G. de Gennes [13] since the situations $H_{c2} < H_c < H_{c3}$ and $H_{c2} < H_{c3} < H_c$ become feasible. In case of a flat surface this corresponds to the ranges $\kappa_c < \kappa < 1/\sqrt{2}$ and $0 < \kappa < \kappa_c$ respectively, where $\kappa_c = 0.417$, which correspond to the *intermediate* ($0.417 < \kappa < 0.707$) and *genuine* ($0 < \kappa < 0.417$) type-I superconductors. The *intermediate* type-I superconductor has a surface state below H_{c3}, which has been discussed by many in the past [24]. For the mesoscopic superconductors this scenario is expected to be richer since the ratio area to volume increases and so the effects of the external surface are enhanced. This study was carried out by L. R. Cadorim et al. [11].

The mesoscopic scale superconductor possesses distinct κ regimes due to its richer critical field structure as compared to the macroscopic scale superconductor. Firstly we review some commonly unknown properties of the critical fields of the macroscopic superconductors that have been stressed by M. Tinkham in his book [12] and experimentally verified long ago [25]. The field H_{c2} is detectable in type-I superconductors through the magnetization, although it falls below H_c. The magnetization, and consequently the order parameter, behaves distinctively for type-I and type-II superconductors. For the type-II superconductors [26] the magnetization shows no special sign at the field H_c. In an isothermal passage from the normal to the superconducting state, the type-II superconductor undergoes a smooth transition at the field H_{c2} since it is a second-order. Distinctively, for the type-I superconductor it is of first order. The normal state remains in *descending* field below the thermodynamic field H_c until the lower field H_{c2} is reached, according to M. Tinkham [12]. There the order parameter abruptly becomes non-zero. In *ascending* field the magnetization remains non zero beyond H_{c2} until H_c is reached, thus completing an hysteresis cycle. However the presence of an external boundary affects the above view because of the field H_{c3}.

In our numerical simulations obtained for the mesoscopic superconductor we have performed field sweeps in *ascending* and *descending* applied field and obtain the isothermal magnetization, $M(H)$. The *ascending* process starts from zero field and the magnetization shows a nearly linear behavior that we refer as the Meissner state until a maximum of $-M(H)$ is reached. This peak defines a critical field called H_c'. Nevertheless the magnetization vanishes and the normal state sets in at another critical field, H_c'', which falls above H_c' ($H_c'' > H_c'$), and the difference between these two fields depends on κ [11]. Notice that H_c' does not coincide with the thermodynamic field H_c, the latter being the bulk field where normal and superconducting states have the same Gibbs free energy in the bulk and H_c' is related with the peak of the magnetization as defined above. The size and the geometry do affect the value of the thermodynamic critical field [27]. The *descending* process starts from an applied field in the normal state. As the field is lowered the superconducting state sets in at the field defined as H_{c3}'. In other words the nucleation of superconductivity in the *descending* process occurs at a critical field lower than the H_c', namely, $H_{c3}' < H_c'$. Therefore remarkably distinct vortex arrangement becomes possible according to κ, giving rise to the distinct type-I regimes studied here. The *descending* magnetization shows jumps within the *intermediate* phase, $\kappa > \kappa_{c1}$, that signal the exit of vortices from the cylinder at each step with a subsequent adjustment to thermodynamical equilibrium. In the range $\kappa < \kappa_{c1}$, the *descending* branch presents an abrupt and vertical growth of the magnetization that characterizes a first order phase transition. This is the *genuine* type-I phase where the spike state sets in, corresponding to a giant vortex at the surface that after being formed is immediately expelled. This remarkable process happens all of a sudden infinitesimally close to H_{c3}' and we determine its lifetime.

Our results are obtained for a very long mesoscopic cylinder with $R = 6\xi$ in presence of an applied field parallel to its major axis for which find that $\kappa_{c1} \approx 0.26$ and $\kappa_{c2} \approx 0.37$. The cylinder is sufficiently long such that the top and the bottom surfaces can be ignored and just a transverse two-dimensional cross section is studied. Besides simplifying the numerical calculation we stress that this geometry is important to avoid the so-called geometrical crossover from the type-I to the type-II superconductor [28–30]. The basic idea behind the geometrical crossover is that a sufficiently thin type-I superconductor becomes a type-II superconductor [31–33] by a change of the thickness (height), w, which causes the effective London penetration to become $\Lambda = \lambda^2/w$ instead of the original λ and this gives an effective GL coupling $\kappa_{eff} = \Lambda/\xi$ that replaces the original one, $\kappa = \lambda/\xi$. The geometrical crossover is not an intrinsic κ transition, and so, it can obscure the observation of the spike state whose onset is associated to the genuine type-I transition observed for $\kappa < \kappa_{c1}$. The geometrical crossover is set by geometry and not by intrinsic material properties.

Our results are obtained by the finite element method and corroborate those obtained using the link variables for a square cross section [11]. However the time evolution discussed here is realistic as compared to previous studies since we use the TDGL theory. Hence the real time evolution of vortex motion inside the superconductor is obtained, and this is very important to characterize the spike state whose visualization is reported here.

Recently an *intermediate* phase was predicted by A. Vagov et al. [34] for a bulk superconductor as a consequence of next order corrections to the standard GL theory carried out in its derivation

from the BCS theory. Their improved GL theory includes the next order corrections and displays a $\kappa - T$ diagram that reveals the onset of an *intermediate* phase between the type-I and II superconductors. This is not the *intermediate* type-I superconductor predicted here, which is a sole consequence of surface effects which are ignored in their approach. Mesoscopic type-I superconductors have been studied both theoretically [8] and experimentally [35], but so far the κ transitions in the mesoscopic scale have not been considered before the work of L. R. Cadorim et al. [11] and the present paper. The emergence of superconductivity in a long mesoscopic cylinder in presence of an applied external field has been studied by G. F. Zharkov et al. [36–39]. Their approach is confined to the search of solutions of the Ginzburg-Landau differential equations with radial symmetry which limits the search to central vortex states. The description of the κ_{c1} and κ_{c2} transition is beyond the scope of their framework since they are limited to a sub set of possible vortex states. In our numerical search, through the finite element method solving the TDGL differential equations, we give a physical description of the spike state. Supercooling and superheating processes have been used as an experimental tool to the study of type-I superconductors [40,41,35] and this method can be easily extended to numerical studies [8]. However the present study is restricted to isothermal processes and instead of supercooling and superheating cycles we study $M(H)$ curves under *ascending* and *descending* applied magnetic field H. Thus the coherence length, $\xi(T)$, is constant at any temperature, T, and so is the length scale set by it.

The outline of this paper is as follows. In Section 2 is presented the time dependent Ginzburg–Landau (TDGL) model used in this article. In Section 3 we report our numerical results that describe the standard expulsion of vortices and also the spike state. We gather our results into a phase diagram. A conclusion is given in Section 4.

2. The model

Since the spike vortex state is a metastable time dependent process that takes place at a single value of the magnetic field, its description requires adequate equations able to describe its evolution. Here we use the standard time dependent Ginzburg-Landau (TDGL) theory for this purpose and to predict the creation and exit of vortices in the superconducting mesoscopic cylinder. Its equations are given below.

$$\frac{\partial \Psi}{\partial t} = -\left(\frac{i}{\kappa}\nabla + \mathbf{A}\right)^2 \Psi + \Psi\left(1 - |\Psi|^2\right), \tag{1}$$

$$\frac{1}{\sigma}\frac{\partial \mathbf{A}}{\partial t} = \mathbf{J} - \nabla \times \nabla \times \mathbf{A}, \tag{2}$$

$$\mathbf{J} = \frac{1}{2i\kappa}\left(\Psi^*\nabla\Psi - \Psi\nabla\Psi^*\right) - |\Psi|^2\mathbf{A}, \tag{3}$$

where $\mathbf{h} = \nabla \times \mathbf{A}$, and $\mathbf{A}$ is the vector potential. Lengths are scaled by the London penetration length, λ, which serves as the unit in our numerical procedure to solve the above equations. Nevertheless, as λ and ξ are connected by $\lambda = \kappa\xi$, where κ is the Ginzburg-Landau coupling, the cylinder has the radius defined by the coherence length, $R = 6\xi$, thus λ changes as we change κ. The time is scaled by the relaxation time given by $\tau = \xi^2/D$ where D is the coefficient of diffusion [42], which is related with the electrical conductivity of the material σ by $D = 1/(\kappa^2\sigma\mu_0)$ [43]. The order parameter, Ψ, is expressed in units of $\Psi_\infty = \sqrt{\alpha/\beta}$, where α and β are the two phenomenological constants defined in the Ginzburg-Landau potential. The magnetic fields, the local ($\mathbf{h}$) and the external applied one ($\mathbf{H}$), are in units of the critical field H_c. Consequently the vector potential $\mathbf{A}$ is in units of λH_c [42,44]. In order to solve the TDGL equations boundary conditions must be imposed, namely, the local and the applied fields are equal at the edge of the sample, i.e., $\nabla \times \mathbf{A}|_{r=R} = \mathbf{H}$, and the super and the normal current cannot pass through the boundary [27,45], $\nabla\Psi \cdot \mathbf{n}|_{r=R} = 0$, and $\mathbf{A} \cdot \mathbf{n}|_{r=R} = 0$, respectively.

The assumption of an infinitely long cylinder simplifies the theoretical treatment since the partial differential equations (1) - (3) must be solved numerically only in two dimensional space. We seek to determine the order parameter, $\Psi(x, y, t)$, and the local magnetic field, $\mathbf{h}(x, y, t) = h_z(x, y, t)\hat{z}$ under an applied field along the z axis, which is the symmetry axis of the cylinder. The numerical simulations solve the above TDGL equations using the finite element method via COMSOL [46,45]. Recently this method was used to solve some bi-dimensional problems on superconductivity under the view of the TDGL theory [46,47,27,45]. The magnetic induction is calculated by $B = \frac{1}{\Omega}\int h(x, y, t_s)d\Omega$, where $d\Omega$ is the element of area of the surface $\Omega = \pi R^2$, where R is the radius of the circular cross section of the long cylinder, t_s is the time after the system reaches the stable configuration. The magnetization is calculated by the usual relation $-4\pi M(H) = B - H$.

3. Results and discussions

In this section we describe the transitions that the mesoscopic type-I superconductors undergo in the coupling κ. For this purpose we discuss the time evolution of the order parameter, Ψ, and of the local magnetic field, $\mathbf{h}$ for the mesoscopic cylinder of radius $R = 6\xi$ for selected Ginzburg-Landau couplings, namely, $\kappa = 0.1$, 0.2, 0.26, 0.28, 0.3, 0.35, 0.36, 0.37, 0.4, 0.42, 0.5, and 0.6. For the *ascending* process the initial state is taken to be $\Psi = 1$ and $H = B = 0$ inside the cylinder. Then H is slowly increased, until superconductivity disappears in the cylinder when the state $\Psi = 0$ and $B = H$ is reached. The *descending* process begins with this state, ($\Psi = 0, B = H$) and H is decreased to zero. Both the standard exit of vortices and the spike state are discussed in the context of the obtained magnetization curves.

In Section 1 we have defined the critical H_c' and H_c'', from the *ascending* branch, and H_{c3}' from the *descending* branch. While the *ascending* branch shows a nearly linear Meissner behavior, the *descending* branch displays jumps related to the vortices, that are expelled as giant vortices and can be regarded as bubbles. The presence of vortices into the cylinder is a fingerprint of an *intermediate* type-I behavior and exists only for a certain κ range, thus revealing the phase transition in κ_{c1}, as previously discussed. The fact that the nucleation of superconductivity occurs at H_{c3}' instead at H_c' is in agreement with M. Tinkham's book [12]. Indeed our notation for this critical fields is inspired by him. The purpose of the present section is to show how vortices are created and how they exit the cylinder, in descending field, changes dramatically according to κ.

3.1. The traditional exit of vortices in descending field

In descending field the passage from the normal to the superconducting state produces the coalescence of the trapped magnetic field into vortices and this is true even for type-I superconductors. While the shielding Meissner supercurrent is diamagnetic, the current of the vortices is paramagnetic. Although a paramagnetic state is expected to arise immediately when the superconducting state sets in, we do not know a priori which of the supercurrents becomes the strongest, and so, whether the magnetization is paramagnetic or diamagnetic. For this reason it is interesting to compute the magnetization for each value of κ. When vortices are formed inside the cylinder, the reduction of the applied field renders the state unstable and their excess is expelled until thermodynamic

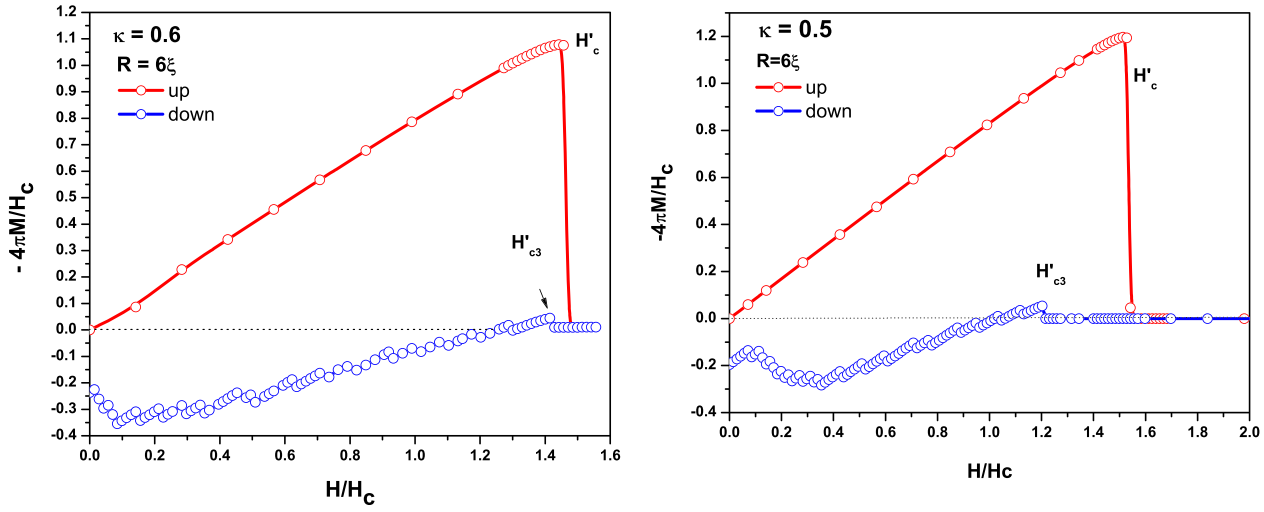

Fig. 1. (Color online.) Magnetization curves for a cylindrical mesoscopic superconductor with radius R = 6ξ and Ginzburg-Landau coupling $\kappa = 0.6$ (left panel) with $H'_c = 1.47H_c$ and $H'_{c3} = 1.41H_c$ and $\kappa = 0.5$ (right panel) with $H'_c = 1.54H_c$ and $H'_{c3} = 1.22H_c$.

equilibrium is restored. We report below these features as obtained by our numerical procedure.

We initially analyze the case $\kappa = 0.6$ as this superconductor falls in the type-I realm since it is below the critical coupling of $\kappa = 1/\sqrt{2}$.

Fig. 1, panel (a), shows the isothermal magnetization curves versus the applied field, $M(H)$, for $\kappa = 0.6$, for both the *ascending* and the *descending* branches, which correspond to the red and blue curves (color online), respectively. The *ascending* $M(H)$ curve shows that the transition to the normal state takes place at $H'_c = 1.47H_c$. The *descending* process shows several jumps in the magnetization, associated to the exit of the quantized vortices from the interior of the cylinder. These jumps are routinely found in case of type-II mesoscopic superconductors [48] and have also been observed in type-I studies [49]. Upon crossing from the normal to the superconducting state, the field inside the cylinder coalesces into a giant vortex. Lowering the field turns this giant vortex unstable and its vorticity must decrease to adjust to the new value of the applied field. The giant vortex decreases its size and also its vorticity during the *descending* process by expelling vortices with vorticity higher than that allowed by thermodynamical equilibrium. The excess vortices are expelled from the cylinder like bubbles, thus we refer to them as vortex bubbles. The presence of hysteresis effects associated to the first order transition that takes place in the normal to superconducting state is clearly seen as we lower the coupling κ. Fig. 1, panel (b) shows the magnetization curves $M(H)$ for a superconducting cylinder with $\kappa = 0.5$. The magnetization behavior is very similar to the last case, however H'_c and H'_{c3} depart from each other. The Meissner state in the *ascending* process collapses when the applied field reaches $H'_c = 1.54H_c$. The *descending* process shows that the nucleation of Ψ and thus the magnetization becomes non zero occurs at $H'_{c3} = 1.22H_c$. Hence, like in the case of $\kappa = 0.6$, the magnetization for the *descending* process is paramagnetic, i.e., $M(H) > 0$, though constrained to a smaller field window.

Fig. 2 brings further understanding to the *ascending* and *descending* processes shown in Fig. 1 through the density $|\Psi|^2$ plotted along the radius of the cylinder. The first and second panels describe the *ascending* and *descending* field sweeps, respectively. The increase of H in the *ascending* process makes $|\Psi|^2$ decrease at the edge of the cylinder although for low fields it is constant at the center of the cylinder. When the applied magnetic field reaches the critical value $H'_c = 1.47H_c$, superconductivity is destroyed throughout the cylinder by an abrupt transition. As an example of our

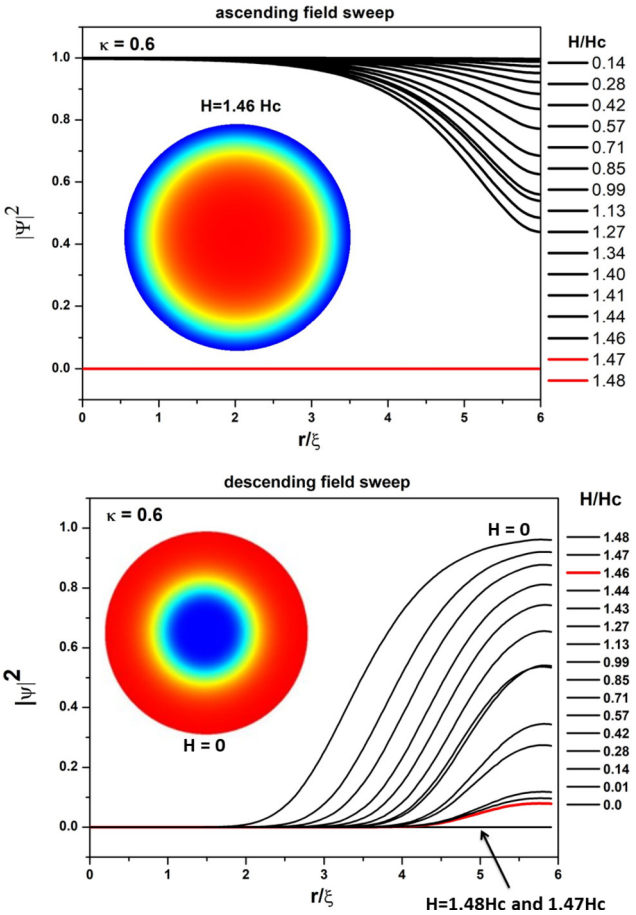

Fig. 2. (Color online.) The superconducting density, $|\Psi|^2$ as function of the radial position, for *ascending* field sweep (top panel) and *descending* field sweep (bottom panel). The Ginzburg-Landau coupling is $\kappa = 0.6$. Increasing the external magnetic field the density vanishes close to the edge of the cylinder and, all of a sudden, when the field reaches $H = H'_c = 1.47H_c$ the superconductivity is totally destroyed. Decreasing the external magnetic field the nucleation of superconductivity occurs when the field reaches $H = H'_{c3} = 1.46H_c$. The inset of the top panel shows the mapping of $|\Psi|^2$ for the applied field just before the phase transition, $H = 1.46H_c$. The inset of the bottom panel shows the mapping of $|\Psi|^2$ when $H = 0$, one can see, the blue color, the presence of a giant vortex in the center of the cylinder.

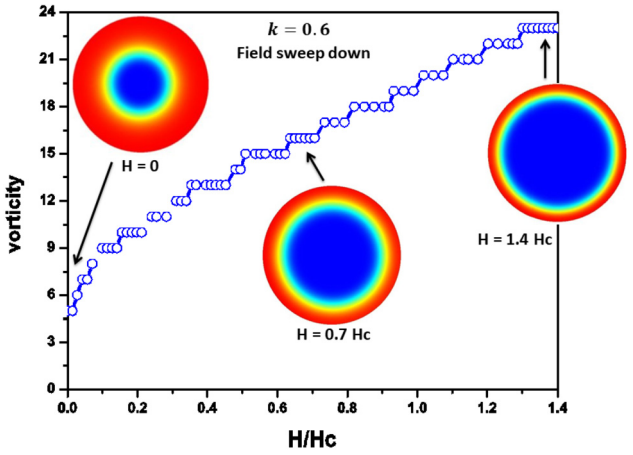

Fig. 3. (Color online.) The vorticity of the system as function of the magnetic field H for the *descending* branch. The GL coupling is $\kappa = 0.6$.

numerical precision, the bottom panel of Fig. 2 shows that, for $H = 1.48H_c$ and $H = 1.47H_c$, the cylinder is still in the normal state, $\Psi = 0$. However for $H = H'_{c3} = 1.46H_c$, suddenly, occurs the nucleation of superconductivity, as seen by the red line in this figure. It is clear that the present configuration describes a giant vortex sitting in the center of the cylinder. Notice that $|\Psi|^2$ is small at the nucleation, and is only present within a rim at the boundary of the cylinder with thickness of the order of ξ. The inset of the top panel of Fig. 2 shows the density contour plot of $|\Psi|^2$ for $H = 1.46H_c$, just before the collapse of superconductivity. Similarly, the inset of the bottom panel shows the density contour plot of $|\Psi|^2$ for $H = 0$.

In summary the exit of vortices for $\kappa = 0.6$ occurs in the standard fashion. Nevertheless we describe it to show the correctness of our numerical procedure and for further comparison with the spike state that arises for $\kappa < \kappa_{c1}$. Fig. 3 shows the decrease of the vorticity as a function of the applied field for the *descending* process. The quantized phase of Ψ is numerically determined, and it reveals the presence of giant vortices inside of the cylinder. It is worth notice that $|\Psi| \neq 0$ is true fundamentally at the edge of the sample and this does not refrain the quantization of the magnetic field confined to the cylinder. Decreasing this magnetic field, makes this giant vortex looses vorticity and consequently, decreases in size. The decrease of the giant vortex core is also seen in Fig. 3.

In case of lower κ regime, new features are observed, as has been pointed out long ago by G. F. Zharkov et al. [36–39,50] and more recently by L. R. Cadorim et al. [11]. Such new features can be observed in Fig. 4, which shows the $M(H)$ curves for both *ascending* and *descending* field sweeps, by showing plots for $\kappa = 0.42$, 0.3, and 0.2. We have selected the value $\kappa = 0.42$ because it corresponds to the *genuine* to *intermediate* type-I transition predicted by M. Tinkham and P. G. de Gennes for a macroscopic interface. For the mesoscopic cylinder, $\kappa = 0.42$ does not correspond to a transition value and just falls in the *paramagnetic-intermediate* regime. While for $\kappa = 0.42$ the descending field magnetization is paramagnetic thus controlled by the exit of vortices, for $\kappa = 0.3$ and $\kappa = 0.2$, we observe a new feature which is a totally diamagnetic magnetization. Still there is a noticeable difference between the $\kappa = 0.3$ and 0.2, which is a discontinuous jump for the former case but not for the latter. This jump is associated to the existence of trapped vortex states which makes us to think that for $\kappa = 0.2$ the vortices have totally disappeared from the cylinder and a genuine type-I superconducting behavior has been reached. However this assertion is not totally true as we show in this paper that for $\kappa = 0.2$ remains the so-called spike state at $H \approx H'_{c3}$.

Fig. 4 shows that the *ascending* field sweep $M(H)$ curves are of a typical type-I behavior for the three cases, and we obtain the field $H'_c = 1.61H_c$, $1.78H_c$, and $2.05H_c$, respectively. For the *descending* field sweep process, no noticeable sign is observed at this field $H = H'_c$, showing that the superconducting state is not sensitive to the H'_c. However decreasing the external magnetic field further on, the nucleation of superconductivity emerges at the upper critical field $H'_{c3} = 0.98H_c$, $0.74H_c$, and $0.43H_c$, respectively. The transition from normal to giant vortex state is a first order phase transition and exemplifies quite well M. Tinkham's claim about the importance of the upper critical field in type-I superconductors. The magnetization curve for $\kappa = 0.42$ presents several jumps starting at $H = H'_{c3}$ until $H = 0$ is reached. The magnetization of the *descending* field sweep process presents a paramagnetic behavior for all superconductors with $1/\sqrt{2} > \kappa > 0.37$. Thus, one can classify these superconductors as *paramagnetic intermediate* type-I superconductors.

3.2. The spike state

In this section we report a detailed analysis of the spike state which is found in the transition from the normal to superconducting state in descending field. This passage seems to be deprived of the presence of vortices for $\kappa \leq \kappa_{c1}$, but this is not so. It contains a vortex state that corresponds to a giant vortex state that is created and immediately leaves the superconductor similar to a spike. This process takes some nanoseconds, as obtained here for Aluminum and it takes place at a single field H'_{c3}. This intense time dependent process is described here through the TDGL theory and depicted in Fig. 6 and Fig. 7 for some time windows. We observe that G. F. Zharkov et al. [36–39,50] have not reported the spike state, because their results are limited to the analysis of central vortices in the context of the time independent GL theory. The description of the spike state can not be achieved by a stable state analysis.

Firstly, we seek to determine in more details the transition *intermediate-genuine* which takes place at κ_{c1}. For this we look the magnetization M versus field H/H_c for $\kappa = 0.26$ and $\kappa = 0.28$, as shown in Fig. 5. M. Tinkham [12] has remarked that the upper critical field, H_{c2}, is observable in macroscopic type-I superconductors and here we find that in the mesoscopic scale the observed field is H'_{c3}. One observes the presence of an intermediate step in panel (b) in comparison to panel (a) that signals a trapped vortex state, that is finally expelled from the cylinder in the traditional fashion. Thus we are facing a transition when going from $\kappa = 0.28$ to $\kappa = 0.26$ which corresponds to the onset of a *genuine* type-I superconductor. Recall that the *intermediate* type-I behavior range defined by Tinkham-de Gennes for macroscopic superconductor, i.e., single planar normal-superconducting interface, is in the range $0.42 < \kappa < 1/\sqrt{2}$. In this work we find that for the mesoscopic superconducting cylinder with radius $R = 6\xi$, this range is found to be $0.27 < \kappa < 1/\sqrt{2}$.

The analysis of the $M(H)$ curves reveals the order of the phase transition. In the *ascending* branch one observes that $H''_c \approx H'_c = 1.87H_c$. The *descending* process starts at $H = 2.0H_c$, where $|\Psi| = 0$ and decreasing H one firstly observes $M \neq 0$ at $H'_{c3} = 0.64H_c$. Although there are no internal jumps in the magnetization curve at this field, since we are below κ_{c2}, the entrance into the superconducting state converts the trapped internal flux into a giant vortex, which is promptly expelled from the volume. This is the spike state.

Figs. 6 and 7 show snapshots of the time evolution of the spike state related to its onset and disappearance. Remarkably, a single vortex state coalesces inside the cylinder at the fixed field of $H = H'_{c3} = 0.64H_c$, and at this very same field, all magnetic field is expelled from the cylinder in form of bubbles of vortices. These

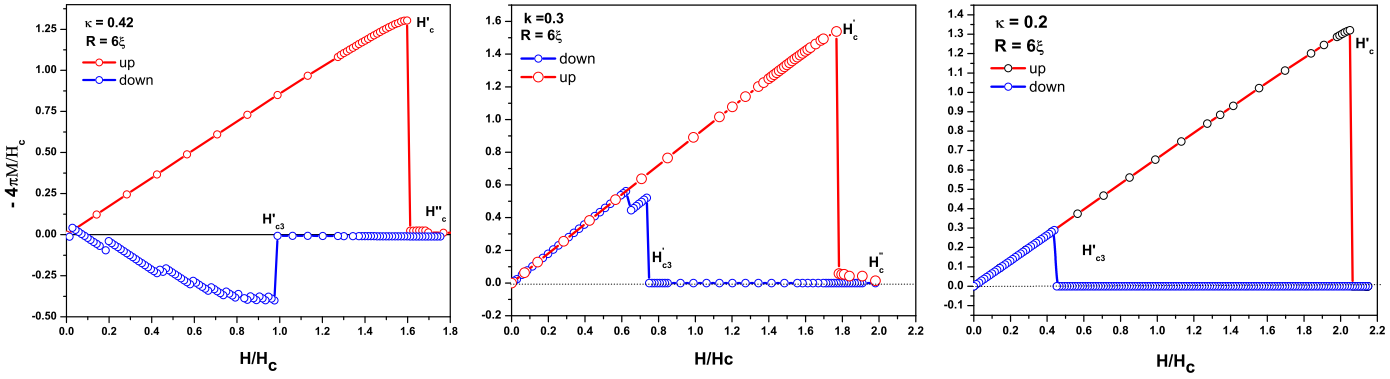

Fig. 4. (Color online.) Magnetization curve for a cylindrical mesoscopic superconductor with radius R = 6ξ. Red line shows the *ascending* field sweep, where a transition occurs at H'_c, and the blue line shows the *descending* field sweep, where the transition takes place at H'_{c3}. We obtain the following transition fields: $\kappa = 0.42$, $H'_c = 1.61H_c$ and $= H'_{c3} = 0.98H_c$; $\kappa = 0.3$, $H'_c = 1.78H_c$ and $H'_{c3} = 0.74H_c$, and $\kappa = 0.2$, $H'_c = 2.05H_c$ and $H'_{c3} = 0.44H_c$.

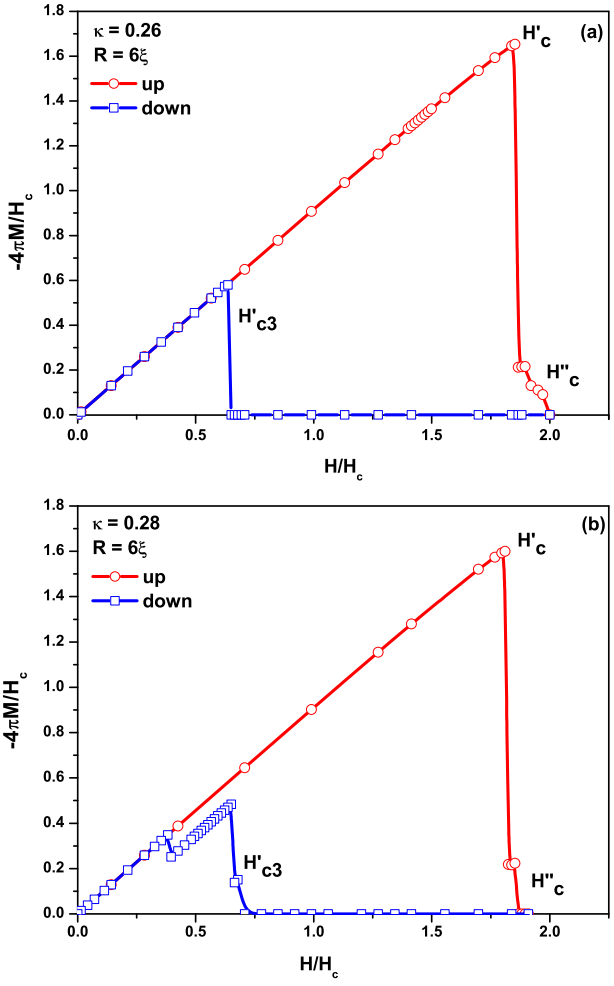

Fig. 5. (Color online.) The magnetization $M(H)$ for a cylindrical mesoscopic superconductor with radius R = 6ξ and Ginzburg-Landau parameter $\kappa = 0.26$ and 0.28. The panels show the field sweep *ascending* in red lines, and the field sweep *descending* in blue lines. Panel (a) shows the magnetization curve for $\kappa = 0.26$, the $H'_c = 1.87H_c$ and $H'_{c3} = 0.64H_c$. Similarly panel (b) shows the magnetization curve for $\kappa = 0.28$, $H'_c = 1.82H_c$ and $H'_{c3} = 0.68H_c$. In the last case, *descending* branch shows steps, and they are related to the exit of giant vortex from the cylinder. In both cases the magnetization is diamagnetic ($M < 0$).

two figures show several snapshots of $|\Psi|^2$, that is, time frames of the time dependent process described by the TDGL equations that takes place at the cylinder. It begins with the normal state at the panel (a) in Fig. 6. The blue color corresponds to the region with low density, $|\Psi|^2 = 0$. The panels (b) and (c) correspond to

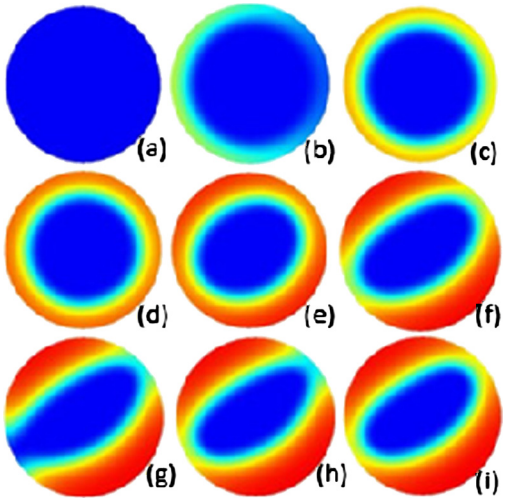

Fig. 6. (Color online.) This sequence shows the initial moments of the nucleation of the spike state inside the cylinder with $\kappa = 0.26$, and thus the formation of the giant vortex at $H'_{c3} = 0.64H_c$. In the first panel, all of the interior is in the normal state, $|\Psi| = 0$.

the starting of the nucleation of $|\Psi|^2$. A giant vortex has been created in the center of the cylinder, as shown in panel (d). Panel (d) describes a radially symmetric state that is not stable and in the subsequent frames this giant vortex undergoes a process of deformation, as shown in panels (e) and (f). Panel (g) shows the first bubble of vortices expelled from the cylinder and panel (h) shows the second expelled bubble, and in panel (i) the order parameter reorganizes itself to form a new but still deformed giant vortex. This process will continue for some time with the expulsion of new vortex bubbles. At this point we jump part of the time evolution to go to Fig. 7, which shows the last snapshots of the giant vortex into the cylinder where the vorticity has been substantially reduced. The panel (a) shows that the giant vortex has become small and close to the edge of the cylinder. In panel (b) one can see the deformation of this vortex along the edge direction, and one vortex bubble is expelled according to panel (c). The panel (d) shows that a reorganization takes place and after a new vortex bubble is expelled, shown in the (e) and (f) panels. The subsequent panels, namely (g), (h), and (i) show new vortex exits. In the bottom line one can observe the last moments of the spike vortex. The panels (j) and (l) show the exit of the last vortex, now reduced to a single vortex. The last panel, (m), shows that the Meissner state is finally reached, and $|\Psi|^2 = 1$ holds inside the cylinder. We have just characterized the vortex dynamics that defines the spike state in the *genuine* type-I superconductor.

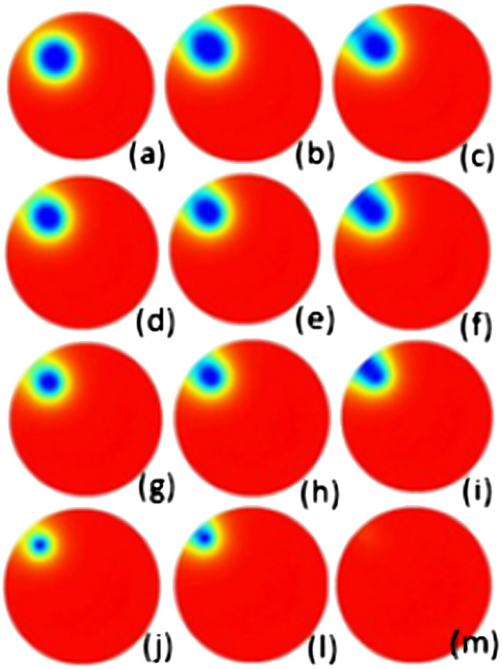

Fig. 7. (Color online.) This sequence shows the last moments of the spike state in the superconducting cylinder with $\kappa = 0.26$. The begin of this process is reported in Fig. 6 and all takes place at the same field value, $H'_{c3} = 0.64H_c$. In the last panel, all of the interior of the cylinder is in Meissner state, $|\Psi| = 1$. The lifetime of this spike state was calculated, $t = 78.8$ ns.

At this point we estimate the lifetime of the spike state for Aluminum (Al). The numerical lifetime of the full process partially reported in Figs. 6 and 7 is $t = 36.000\tau$ where τ is the time unit defined by the TDGL theory. For Aluminum, the coherence length is $\xi = 1600$ nm, the London penetration length is $\lambda = 16$ nm, the GL coupling $\kappa = 0.01$ [51]. The normal-state resistivity at low temperature is $\rho = 10^{-9}\ \Omega \cdot$ m [52]. Thus, the Aluminum diffusion coefficient is $D = 1.17\ \mathrm{m}^2/\mathrm{s}$, the relaxation time is $\tau = 2.19$ ps, and the lifetime of the spike state is found to be $t = 78.8$ ns. The extremely low value of κ for Aluminum can be increased and adjusted by the inclusion of impurities. This allows us to change this parameter without altering the height and the cross section of the needles. The proposal of a long needle oriented along the applied field makes us consider the Aharonov-Bohm effect as a way to detect the spike state [53]. The spike state could also be detected by using microwave radiation which was used to measure the velocity of super-fast kinematic vortices in Pb thin superconducting films [7].

3.3. The phase diagram

In this Section, we construct the diagram κ versus the applied field H for the mesoscopic superconducting cylinder with a fixed radius, $R = 6\xi$, and show its several possible regimes. Notice that each simulation is performed without changing the value of κ. Interestingly, for $\kappa < 0.37$, both, ascending and descending branches present $M < 0$, thus $\kappa_{c2} = 0.37$. In Fig. 4, the center and right panels show diamagnetic behavior, different from the cases shown for $\kappa > 0.37$. Thus these superconductors can be classified as *diamagnetic-intermediate* Type-I superconductors. The study of the magnetization curves $M(H)$ for selected values of κ, as done here, makes possible to determine how the critical fields H'_c and H'_{c3} depend on κ.

Fig. 8 shows this diagram and its properties, and reveals the decrease of H'_c and the increase of H'_{c3} with respect to κ. Recall that H'_c is determined in the *ascending* branch, and so, above this line

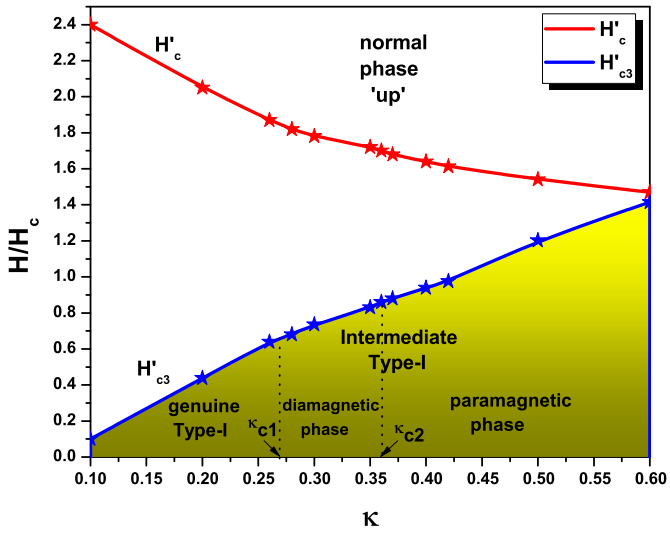

Fig. 8. (Color online.) $H - \kappa$ diagram for the superconducting cylinder with radius $R = 6\xi$. The dotted line at κ_{c1} divides this diagram in two main parts, *genuine* type-I superconductors for $\kappa < \kappa_{c1}$, and *Intermediate* type-I superconductors for $\kappa > \kappa_{c1}$. The last phase is also divided in two parts, the dashed line at k_{c2} separates the diamagnetic phase for $\kappa_{c1} < \kappa < \kappa_{c2}$, and the paramagnetic phase for $\kappa_{c2} < \kappa < \kappa_c$. The spike state is present just for $\kappa < \kappa_{c1}$, i.e., in the transition from the normal to *genuine* type-I superconductors phase.

($H > H'_c$) the normal state is restored and below it ($H < H'_c$), is the Meissner state. The field H'_{c3} is determined in the *descending* branches, and so, above this line ($H > H'_{c3}$) we have the normal state. Nevertheless below this line ($H < H'_{c3}$) there are two regimes, namely, the *Giant vortex phase 'down'* for $\kappa_{c1} \leq \kappa \leq 0.6$ ($\kappa = 0.6$ is the upper limit carried in our simulations) and the *Meissner phase 'down'* for $\kappa < \kappa_{c1}$. $\kappa_{c1} = 0.27$ sets the transition between the *genuine* and the *intermediate* type-I superconductors. For $\kappa_{c1} < 0.27$ one naively expects no entrance or exit of vortices in descending field, but this is not so. In fact in this case we report here the existence of a spike vortex state.

Notice that the signal of $M(H)$ reveals important information about the κ transitions. Notice that regardless of κ the *ascending* branch shows a diamagnetic magnetization, $M < 0$. Nevertheless for the *descending* branch the magnetization changes its signal as the coupling κ is changed. For $\kappa < \kappa_{c2} = 0.37$ the magnetization is diamagnetic while for $\kappa > \kappa_{c2} = 0.37$ it is paramagnetic, $M > 0$. These two different magnetic responses signal the existence of three phases of mesoscopic type-I superconductors, the *genuine* for $\kappa < \kappa_{c1}$, the *diamagnetic-intermediate* for $\kappa_{c1} < \kappa < \kappa_{c2}$, and finally, the *paramagnetic intermediate* type-I superconductors, for $\kappa_{c2} \leq \kappa \leq 0.6$.

4. Conclusions

In this paper we study the spike state, which is another example of a metastable vortex state like the phase slips centers and phase slip lines. The study is done in the context of the time dependent Ginzburg-Landau equations applied in case of a long cylinder with radius $R = 6\xi$, subjected to an external magnetic field along its symmetry axis. We contextualize the spike state within the general study of κ transitions in mesoscopic superconductors proposed by L. R. Cadorim et al. [11]. These transitions require that, both *ascending* and *descending* sweeps of the applied magnetic field must be studied in order to determine the rich magnetic phases of the mesoscopic type-I superconductors. In the former case the initial state is at $\Psi = 1$ and $\mathbf{B} = 0$ and the field is slowly increased until the normal state is reached. In the latter case the cylinder begins at the normal state with $\Psi = 0$ and the magnetic field is homogeneous inside its interior. The field is

then slowly decreased until $H = 0$ is reached. For the *ascending* process, the magnetization curves present a nearly linear growth for increasing field, which is the typical type-I behavior for all the values of κ studied here. However, for the *descending* process, the superconducting cylinder with κ coupling falling in the range $\kappa_{c1} = 0.27 < \kappa < 1/\sqrt{2}$ presents jumps in the magnetization. These jumps set the exit of vortices from the cylinder and happen for the class of *intermediate* type-I superconductors. The expulsion of the magnetic field from the cylinder, during the *descending* process, occurs via bubbles of vortices. The jumps are absent for $\kappa < \kappa_{c1}$. This characterizes the *genuine* type-I superconductor. Nevertheless, at the fixed field $H = H'_{c3}$, when the cylinder becomes superconductor, we find the spike state, as shown in Fig. 6 and Fig. 7 for the selected time frames. The TDGL simulation allows to estimate the lifetime of this spike state which is found to fall in the nanosecond range for Aluminum.

CRediT authorship contribution statement

I.G. de Oliveira – Idea, numerical simulations, discussions and writing. L.R. Cadorim – Discussions and revision. A.R. de C. Romaguera – Discussions and revision. E. Sardella – Discussions and revision. R.R. Gomes – Discussions and revision. M.M. Dória – Idea, discussions and writing.

Declaration of competing interest

The authors declare that they have no known competing financial interests or personal relationships that could have appeared to influence the work reported in this paper.

Acknowledgements

L.R. Cadorim thanks the Brazilian Agency CAPES for financial support (process number 88887.494140/2020-00). I. G. de Oliveira and M. M. Dória thank the Brazilian Agency Fundação de Amparo Pesquisa do Estado do Rio de Janeiro (FAPERJ) for financial support with process No. E-26/010.001497/2019. L. R. Cadorim thanks Brazilian Agency FAPESP for financial support (process number 20/03947-2), A. R. de C. Romaguera, M. M. Dória e E. Sardella thank FACEPE and CAPES for financial support with the project number APQ-0198-1.05/14. E. Sardella thanks the Brazilan Agency FAPESP for financial support (process number 20/10058-0).

References

[1] W.W. Webb, R.J. Warburton, Intrinsic quantum fluctuations in uniform filamentary superconductors, Phys. Rev. Lett. 20 (1968) 461–465, https://doi.org/10.1103/PhysRevLett.20.461, https://link.aps.org/doi/10.1103/PhysRevLett.20.461.

[2] W.A. Little, Decay of persistent currents in small superconductors, Phys. Rev. 156 (1967) 396–403, https://doi.org/10.1103/PhysRev.156.396, https://link.aps.org/doi/10.1103/PhysRev.156.396.

[3] J.S. Langer, V. Ambegaokar, Intrinsic resistive transition in narrow superconducting channels, Phys. Rev. 164 (1967) 498–510, https://doi.org/10.1103/PhysRev.164.498, https://link.aps.org/doi/10.1103/PhysRev.164.498.

[4] D.E. McCumber, B.I. Halperin, Time scale of intrinsic resistive fluctuations in thin superconducting wires, Phys. Rev. B 1 (1970) 1054–1070, https://doi.org/10.1103/PhysRevB.1.1054, https://link.aps.org/doi/10.1103/PhysRevB.1.1054.

[5] I. Petković, A. Lollo, L.I. Glazman, J.G.E. Harris, Deterministic phase slips in mesoscopic superconducting rings, Nat. Commun. 7 (1) (2016) 13551, https://doi.org/10.1038/ncomms13551.

[6] N. Paradiso, A.-T. Nguyen, K.E. Kloss, C. Strunk, Phase slip lines in superconducting few-layer NbSe 2 crystals, 2D, Materials 6 (2) (2019) 025039, https://doi.org/10.1088/2053-1583/ab0bcc.

[7] A.G. Sivakov, A.M. Glukhov, A.N. Omelyanchouk, Y. Koval, P. Müller, A.V. Ustinov, Josephson behavior of phase-slip lines in wide superconducting strips, Phys. Rev. Lett. 91 (2003) 267001, https://doi.org/10.1103/PhysRevLett.91.267001, https://link.aps.org/doi/10.1103/PhysRevLett.91.267001.

[8] G.R. Berdiyorov, M.V. Milošević, F.M. Peeters, Tunable kinematics of phase-slip lines in a superconducting stripe with magnetic dots, Phys. Rev. B 80 (2009) 214509, https://doi.org/10.1103/PhysRevB.80.214509, https://link.aps.org/doi/10.1103/PhysRevB.80.214509.

[9] G.R. Berdiyorov, A.R. de, C. Romaguera, M.V. Milošević, M.M. Doria, L. Covaci, F.M. Peeters, Dynamic and static phases of vortices under an applied drive in a superconducting stripe with an array of weak links, Eur. Phys. J. B 85 (4) (2012) 130, https://doi.org/10.1140/epjb/e2012-30013-7.

[10] L. Embon, Y. Anahory, Ž.L. Jelić, E.O. Lachman, Y. Myasoedov, M.E. Huber, G.P. Mikitik, A.V. Silhanek, M.V. Milošević, A. Gurevich, E. Zeldov, Imaging of super-fast dynamics and flow instabilities of superconducting vortices, Nat. Commun. 8 (1) (2017) 85, https://doi.org/10.1038/s41467-017-00089-3.

[11] L.R. Cadorim, A.R.d.C. Romaguera, I.G. de Oliveira, R.R. Gomes, M.M. Doria, E. Sardella, Intermediate type-i superconductors in the mesoscopic scale, Phys. Rev. B 103 (2021) 014504, https://doi.org/10.1103/PhysRevB.103.014504, https://link.aps.org/doi/10.1103/PhysRevB.103.014504.

[12] T. Michael, Introduction to Superconductivity, 2nd edition, Dover Publication, New York, 2008.

[13] P. De Gennes, Superconductivity of Metals and Alloys, Frontiers in Physics, Benjamin, 1966, https://books.google.com.br/books?id=KtJEAAAAIAAJ.

[14] A.A. Abrikosov, Sov. Phys. JETP 5 (1957) 1174–1178.

[15] E.B. Bogomolny, Sov. J. Nucl. Phys. 24 (1976) 449–454.

[16] I. Luk'yanchuk, Theory of superconductors with κ close to $1/\sqrt{2}$, Phys. Rev. B 63 (2001) 174504, https://doi.org/10.1103/PhysRevB.63.174504, https://link.aps.org/doi/10.1103/PhysRevB.63.174504.

[17] D. Saint-James, P. Gennes, Onset of superconductivity in decreasing fields, Phys. Lett. 7 (5) (1963) 306–308, https://doi.org/10.1016/0031-9163(63)90047-7, http://www.sciencedirect.com/science/article/pii/0031916363900477.

[18] D. Saint-James, Etude du champ critique hc3 dans une geometrie cylindrique, Phys. Lett. 15 (1) (1965) 13–15, https://doi.org/10.1016/0031-9163(65)91101-7, http://www.sciencedirect.com/science/article/pii/0031916365911017.

[19] K. Kwasnitza, G. Rupp, Measurement of critical field hc3 and critical surface current in superconducting v-ti alloys up to 30 koe, Phys. Lett. 23 (1966) 40–42, https://doi.org/10.1016/0031-9163(66)90247-2.

[20] J. Hauser, J.-Y. Wang, C. Kittel, Calculation of the surface critical field hc3 for a cylindrical cavity, Phys. Lett. A 47 (1) (1974) 34–36, https://doi.org/10.1016/0375-9601(74)90094-2, http://www.sciencedirect.com/science/article/pii/0375960174900942.

[21] I.N. Askerzade, Surface critical magnetic field hc3(t) of a bulk superconductor mgb2 using two-band Ginzburg-Landau theory, Pramana 61 (3) (2003) 611–616, https://doi.org/10.1007/BF02705483.

[22] A. Changjan, S. Meakniti, P. Udomsamuthirun, The temperature-dependent surface critical magnetic field (hc3) of magnetic superconductors: applied to lead bismuth (pb82bi18) superconductors, J. Phys. Chem. Solids 107 (2017) 32–35, https://doi.org/10.1016/j.jpcs.2017.03.022, http://www.sciencedirect.com/science/article/pii/S0022369716313592.

[23] H.-Y. Xie, V.G. Kogan, M. Khodas, A. Levchenko, Onset of surface superconductivity beyond the Saint-James–de Gennes limit, Phys. Rev. B 96 (2017) 104516, https://doi.org/10.1103/PhysRevB.96.104516, https://link.aps.org/doi/10.1103/PhysRevB.96.104516.

[24] J. Feder, Comments of the supercooling field for superconductors with k values near 0.4, Solid State Commun. 5 (4) (1967) 299–301, https://doi.org/10.1016/0038-1098(67)90277-3, http://www.sciencedirect.com/science/article/pii/0038109867902773.

[25] J. Feder, D.S. McLachlan, Superheating and supercooling in single spheres of tin, indium, and gold-plated indium, Phys. Rev. 177 (1969) 763–776, https://doi.org/10.1103/PhysRev.177.763, https://link.aps.org/doi/10.1103/PhysRev.177.763.

[26] M.M. Doria, S. Salem-Sugui, I.G. de Oliveira, L. Ghivelder, E.H. Brandt, Average kinetic energy of the superconducting state, Phys. Rev. B 65 (2002) 144509, https://doi.org/10.1103/PhysRevB.65.144509, https://link.aps.org/doi/10.1103/PhysRevB.65.144509.

[27] I.G. de Oliveira, The threshold temperature where type-I and type-II interchange in mesoscopic superconductors at the Bogomolnyi limit, Phys. Lett. A 381 (14) (2017) 1248–1254, https://doi.org/10.1016/j.physleta.2017.01.032, http://www.sciencedirect.com/science/article/pii/S0375960117300750.

[28] W.Y. Córdoba-Camacho, R.M. da Silva, A. Vagov, A.A. Shanenko, J.A. Aguiar, Between types I and II: intertype flux exotic states in thin superconductors, Phys. Rev. B 94 (2016) 054511, https://doi.org/10.1103/PhysRevB.94.054511, https://link.aps.org/doi/10.1103/PhysRevB.94.054511.

[29] W.Y. Córdoba-Camacho, R.M. da Silva, A. Vagov, A.A. Shanenko, J.A. Aguiar, Quasi-one-dimensional vortex matter in superconducting nanowires, Phys. Rev. B 98 (2018) 174511, https://doi.org/10.1103/PhysRevB.98.174511, https://link.aps.org/doi/10.1103/PhysRevB.98.174511.

[30] W.Y. Córdoba-Camacho, R.M. da Silva, A.A. Shanenko, A. Vagov, A.S. Vasenko, B.G. Lvov, J.A. Aguiar, Spontaneous pattern formation in superconducting films, J. Phys. Condens. Matter 32 (7) (2019) 075403, https://doi.org/10.1088/1361-648x/ab5379.

[31] R.D. Parks, J.M. Mochel, Evidence for quantized vortices in a superconducting strip, Phys. Rev. Lett. 11 (1963) 354–358, https://doi.org/10.1103/PhysRevLett.11.354, https://link.aps.org/doi/10.1103/PhysRevLett.11.354.

[32] M. Tinkham, Effect of fluxoid quantization on transitions of superconducting films, Phys. Rev. 129 (1963) 2413–2422, https://doi.org/10.1103/PhysRev.129.2413, https://link.aps.org/doi/10.1103/PhysRev.129.2413.

[33] J. Pearl, Current distribution in superconducting films carrying quantized fluxoids, Appl. Phys. Lett. 5 (4) (1964) 65–66.
[34] A. Vagov, A.A. Shanenko, M.V. Milošević, V.M. Axt, V.M. Vinokur, J.A. Aguiar, F.M. Peeters, Superconductivity between standard types: multiband versus single-band materials, Phys. Rev. B 93 (2016) 174503, https://doi.org/10.1103/PhysRevB.93.174503, https://link.aps.org/doi/10.1103/PhysRevB.93.174503.
[35] A. Müller, M.V. Milošević, S.E.C. Dale, M.A. Engbarth, S.J. Bending, Magnetization measurements and Ginzburg-Landau simulations of micron-size β-tin samples: evidence for an unusual critical behavior of mesoscopic type-I superconductors, Phys. Rev. Lett. 109 (2012) 197003, https://doi.org/10.1103/PhysRevLett.109.197003, https://link.aps.org/doi/10.1103/PhysRevLett.109.197003.
[36] G.F. Zharkov, V.G. Zharkov, A.Y. Zvetkov, Ginzburg-Landau calculations for a superconducting cylinder in a magnetic field, Phys. Rev. B 61 (2000) 12293–12301, https://doi.org/10.1103/PhysRevB.61.12293, https://link.aps.org/doi/10.1103/PhysRevB.61.12293.
[37] G.F. Zharkov, Paramagnetic Meissner effect in superconductors from self-consistent solution of Ginzburg-Landau equations, Phys. Rev. B 63 (2001) 214502, https://doi.org/10.1103/PhysRevB.63.214502, https://link.aps.org/doi/10.1103/PhysRevB.63.214502.
[38] G.F. Zharkov, On the emergence of superconductivity and hysteresis in a cylindrical type I superconductor, J. Exp. Theor. Phys. 95 (3) (2002) 517–525, https://doi.org/10.1134/1.1513826.
[39] G.F. Zharkov, First and second order phase transitions and magnetic hysteresis in a superconducting plate, J. Low Temp. Phys. 130 (1) (2003) 45–67, https://doi.org/10.1023/A:1021845418088.
[40] J. Park, Metastable states of the superconducting surface sheath in decreasing fields, Solid State Commun. 5 (8) (1967) 645–648, https://doi.org/10.1016/0038-1098(67)90084-1, http://www.sciencedirect.com/science/article/pii/0038109867900841.
[41] J. McEvoy, D. Jones, J. Park, Supercooling of superconductors below the surface nucleation field, Solid State Commun. 5 (8) (1967) 641–644, https://doi.org/10.1016/0038-1098(67)90083-X, http://www.sciencedirect.com/science/article/pii/003810986790083X.
[42] W.D. Gropp, H.G. Kaper, G.K. Leaf, D.M. Levine, M. Palumbo, V.M. Vinokur, Numerical simulation of vortex dynamics in type-II superconductors, J. Comput. Phys. 123 (2) (1996) 254–266.
[43] T. Winiecki, C.S. Adams, Time-dependent Ginzburg-Landau simulations of the voltage-current characteristic of type-ii superconductors with pinning, Phys. Rev. B 65 (2002) 104517, https://doi.org/10.1103/PhysRevB.65.104517, https://link.aps.org/doi/10.1103/PhysRevB.65.104517.
[44] L.P. Gor'kov, G.M. Éliashberg, Generalization of the Ginzburg-Landau equations for non-stationary problems in the case of alloys with paramagnetic impurities, Sov. Phys. JETP 27 (1968) 328.
[45] T.S. Alstrøm, M.P. Sørensen, N.F. Pedersen, S. Madsen, Magnetic flux lines in complex geometry type-II superconductors studied by the time dependent Ginzburg-Landau equation, Acta Appl. Math. 115 (1) (2011) 63–74, https://doi.org/10.1007/s10440-010-9580-8.
[46] I.G. de Oliveira, Magnetic flux penetration in a mesoscopic superconductor with a slit, J. Supercond. Nov. Magn. 27 (5) (2014) 1143–1152, https://doi.org/10.1007/s10948-013-2390-2.
[47] I.G. de Oliveira, Instability in the magnetic field penetration in type-II superconductors, Phys. Lett. A 379 (22) (2015) 1486–1491, https://doi.org/10.1016/j.physleta.2015.03.032, http://www.sciencedirect.com/science/article/pii/S0375960115003072.
[48] V.A. Schweigert, F.M. Peeters, Phase transitions in thin mesoscopic superconducting disks, Phys. Rev. B 57 (1998) 13817–13832, https://doi.org/10.1103/PhysRevB.57.13817, https://link.aps.org/doi/10.1103/PhysRevB.57.13817.
[49] J. Ge, J. Gutierrez Royo, B. Raes, J. Cuppens, V. Moshchalkov, Flux pattern transitions in the intermediate state of a type-i superconductor driven by an ac field, New J. Phys. 15 (2013) 033013, https://doi.org/10.1088/1367-2630/15/3/033013.
[50] G.F. Zharkov, Superconducting states of the cylinder with a single vortex in magnetic field according to the Ginzburg-Landau theory, Cent. Eur. J. Phys. 3 (1) (2005) 77, https://doi.org/10.2478/BF02476508.
[51] C. Kittel, Introduction to Solid State Physics, 6th edition, John Wiley & Sons, Inc., New York, 1986.
[52] P. Duthil, Material properties at low temperature, in: Proceedings of CAS - CERN Accelerator School: Course on Superconductivity for Accelerators, European Organization for Nuclear Research (CERN), 2014, p. 592, Materials Science, arXiv:1501.07100.
[53] Y. Aharonov, D. Bohm, Significance of electromagnetic potentials in the quantum theory, Phys. Rev. 115 (1959) 485–491, https://doi.org/10.1103/PhysRev.115.485, https://link.aps.org/doi/10.1103/PhysRev.115.485.